Postcranial evidence of late Miocene hominin bipedalism in Chad

Franck Guy, Guillaume Daver, Hassane Taisso Mackaye, Andossa Likius, Jean-Renaud Boisserie, Abderamane Moussa, Patrick Vignaud, Clarisse Nekoulnang

Article

Postcranial evidence of late Miocene hominin bipedalism in Chad.

Daver G.[1,*], Guy F.[1,*], Mackaye H. T.[2], Likius A.[2,3], Boisserie J.R.[1,4], Moussa A.[2], Vignaud P.[1], Nekoulnang C[5].

*** Daver G. & Guy F. contributed equally to this work and are both considered first authors.**

1. PALEVOPRIM : Laboratoire de Paléontologie, Evolution, Paléoécosystèmes et Paléoprimatologie. Université de Poitiers, CNRS, F-86073. Poitiers, France.
2. Université de N'Djamena - Faculté de Sciences Exactes et Appliquées -Département de Paléontologie BP 1117 - N'Djamena – TCHAD
3. Académie de l'Education Nationale du Nord, Faya, BP 1117, N'Djaména, Tchad;
4. CFEE: Centre Français des Etudes Ethiopiennes. CNRS and French Ministry of Europe and foreign affairs, PO Box 5554, Addis Ababa, Ethiopia.
5. Centre National de Développement et de la Recherches (CNRD) - Service de Conservation et Valorisation des Fossiles - BP 1228 - N'Djamena - TCHAD

Terrestrial bipedal locomotion is one of the key adaptations defining the hominin clade. Evidences of undisputed bipedalism are known from postcranial remains of late Miocene hominins as soon as 6 Ma in eastern Africa. Bipedality of *Sahelanthropus tchadensis* was hitherto documented at 7 Ma in central Africa (Chad) by cranial evidence. Here, we present the first postcranial evidence of the locomotor behavior of the Chadian hominin with new insights on bipedalism at the early stage of our evolutionary history. The original material was discovered at locality TM 266 (Toros-Menalla fossiliferous area), and consists in one left femur and two antimeric ulnae. These new findings confirm that hominins were already terrestrial biped relatively soon after the human-chimpanzee divergence but also suggest that careful climbing arboreal behaviors was still a significant part of their locomotor repertoire.

Discoveries in Chad by the Mission Paleoanthropological Franco-Tchadienne (MPFT) have substantially contributed to our understanding of early human evolution in Africa. The locality TM 266 (Extended data 1) in the Toros-Menalla fossiliferous area in the Mega-Chad basin yielded, among hundreds of vertebrate remains, a nearly complete cranium (TM 266-01-60-1), three mandibles, and several isolated teeth depicting a minimum of three adult individuals assigned to *Sahelanthropus tchadensis*[1,2]. TM 266 fossils were found in the Anthracotheriid Unit with biochronological estimates and radiochronological age at ca. 7 Ma[3,4]. Environmental indicators at Toros-Menalla localities, at the time, suggested a lacustrine fringe, in a desert vicinity, where open areas with dry and humid grasslands coexisted with arboreal cover[5,6].

Three other hominin fossil remains were discovered at TM 266 in 2001 by the MPFT: one left femoral shaft (TM 266-01-063, unearthed in July 2001), and two right and left ulnae (respectively TM 266-01-358, unearthed in November 2001 and TM 266-01-050, unearthed in July 2001; Supplementary notes). Despite none of these limb bones can be reliably ascribed to any hominin craniodental specimen found at TM 266, the most parsimonious hypothesis is that these postcranial remains belong to the sole hominin species present in this locality. Hence, we favor a conservative attribution of these specimens to *Sahelanthropus tchadensis*.

The hindlimb is documented by a left femoral shaft (TM 266-01-063) of about 242 mm long (Fig. 1 and Supporting table 1, Extended data 2), lacking the distal epiphysis and most of the proximal one. The specimen is curved anteroposteriorly as in *Australopithecus*[7-9] and *Orrorin tugenensis* (BAR 1002'00 and BAR 1003'00) but more heavily built. The two major mediolateral axes of the proximal and distal diaphyseal portions clearly indicate that the neck must have been anteverted as in fossil hominins[9-11] (Extended data 3). The presence of a groove on the postero-superior surface of the

neck for the *obturator internus* and *m. gemelli* supports this interpretation. Resulting in head/neck torsion relative to the long axis of the shaft[12].This condition is also reported in archaic fossil apes such as *Nacholapithecus* and *Ekembo* but is absent in the arboreal biped *Danuvius*[13]. The femur exhibits proximal platymeria just distal to the lesser trochanter (Supplementary notes), a trait encountered in *O. tugenensis* and later hominins and suggested to correlate with neck elongation, a reliable indicator of hominin bipedalism[9,14-16] (but see [8,17]). Concurrently, the neck is compressed antero-posteriorly as in the Miocene ape *Danuvius guggenmosi*[13] and hominins[8-9,18] (but see [19] for *Dryopithecus fontani* and *Hispanopithecus laietanus*; Fig. 1). This array of features agrees with habitual bipedalism in *S. tchadensis*.

A small but sharp relief, indicative of the third trochanter, continues into a rugose surface distally and blends with the lateral component of a broad 'proto-*linea aspera*'[17] (12.2mm in its narrowest width). The lateral lip of the *linea* forms a well-marked sigmoid line. Similarly, the medial lip of the *linea aspera* is well-marked. The spiral line for the insertion of the *vastus medialis* consists in a straight line, which confounds distally with the medial lip of the *linea aspera*. Such configuration is also observed in *O. tugenensis* and *Ardipithecus ramidus*[8,16,18] albeit with a more salient 'proto-linea aspera' in TM 266-01-063, but differs from modern humans where a pilaster develops. Such an overall pattern is consistent with bipedalism albeit suggesting a less-developed quadriceps system relative to the hamstring compared to modern human-like pattern[17].

The femoral shaft exhibits thick cortical bone in cross-section (Fig. 2). Cortical thickness distribution pattern describes a posterior and lateral thickening of the diaphysis relative to an anterior and medial thinning (Fig. 3). Posterior thickening of the cortical bone occurs at the level of the nutrient foramen, where the 'proto-*linea aspera*' is the narrowest. Conversely, extant apes share a posterior thickening on proximal half of the shaft and a relative thinning on distal half[20] (see also Supporting Information in [21]). Lateral thickening can be traced on the major part of the shaft in TM 266-01-063 except in its most distal portion. African apes do not display extended lateral thickening but instead, a circumscribed thickening corresponding to the lateral spiral pilaster. In these aspects, TM 266-01-063 most resembles extant humans. Comparative data are, to our knowledge, inexistent for *Ardipithecus*. Besides, cortical thickness data reported for BAR 1002'00 (*O. tugenensis)* rely on CT-scan data whose reliability is questionable[22-24].

Cortical area and second moment of area (I_x/I_y and I_{max}/I_{min}) are biomechanical parameters frequently used to infer habitual locomotor functions in primates, as they reflect loads undergone by long bones during growth (but see [25]). The cortical area of the diaphyseal cross-section is a measure of resistance of the bone to axial compression or tension, while second moment of area measures the resistance to bending loads. In TM 266-01-063, percent of cortical area is 66.5 % at the level of the nutrient foramen (see Methods) and slightly increase proximally. It is within the range of extant and fossil apes (75 % ± 3.6 in extant humans; 63.3 % ± 7.6 in chimpanzees; 70 % ± 3.9 in gorillas;

Supporting Information in [21]) and above the value reported for AL 288-1 femur (59.9 %) at midshaft[26]. Response to bending loads endured by the femur from TM 266 is assessed at the level of the nutrient foramen using second moment of area[26,27]. Results for I_{max}/I_{min} and I_x/I_y are respectively 1.31 and 0.81 (Extended data 4). The Chadian femur approaches the chimpanzee/extant human condition in its Imax/Imin ratio (measured at midshaft[28,29]; humans, I_{max}/I_{min}=1.6 ± 0.36; chimpanzees, Imax/Imin=1.4 ± 0.2) whereas it departs from gorillas[28] (I_{max}/I_{min}=1.9 ± 0.3). The I_x/I_y of TM 266-01-063 is close to values reported for chimpanzees (chimpanzee[30]: I_x/I_y=0.75 ± 0.08), early *Homo*[31-33] and early to Middle Pleistocene hominins[34]. It departs from extant humans in which a posterior pilaster develops[29] (I_x/I_y =1.52 ± 0.39). Whereas midshaft cross-section of TM 266-01-063 resembles in its overall aspect to AL 288-1, the Chadian specimen present higher I_{max}/I_{min} and lower I_x/I_y values than its younger eastern-African relative (*A. afarensis*: AL 288-1[26], I_x/I_y=0.98 and I_{max}/I_{min}=1.07; see also [35] for AL 333-61, I_x/I_y=1.16 and I_{max}/I_{min}=1.16).

Many aspects such as stature, body mass, muscle attachment sites, positional behavior, ontogeny and sexual dimorphism[25] may contribute to femoral bone mass distribution. Yet, geometry of the TM 266-01-063 indicates greatest bending resistance for medio-laterally oriented stresses. This condition seen in AL 288-1 and early African and Asian *Homo* is suggested to relate to a more lateral position of the body during the stance phase of gait in association with an increase in femoral neck length and biacetabular breadth[26]. Functional interpretations remain difficult to formulate given the paucity of early hominin comparative data and given the state of preservation of the Chadian femur. Nevertheless, the Chadian femoral shaft exhibits a well-developed *calcar femorale* (CF) in its proximal portion (Fig. 4; the CF is 18.80 mm long measured at the level of the lesser trochanter following[36]), a condition to date only seen in extant humans and reported in *O. tugenensis* (BAR 1003'00). The *calcar femorale* corresponds to a bony wall that originates from the postero-medial endosteal surface at the level of the lesser trochanter and extends laterally toward the greater trochanter. In obligate bipeds, it facilitates compressive loads dispelling in the proximal femur by decreasing the stress in the posterior and medial aspects and increasing the stress in the anterior and lateral aspects[36,37]. A well-developed *calcar femorale* in TM 266-01-063 represents a morphological requirement for terrestrial bipedalism.

The forearm bones attributed to *Sahelanthropus tchadensis* consist in two partial left and right ulnae lacking the distal epiphyses. Similarity in size and shape for the antimeric ulnae could suggest they are from the same individual, even if no definitive evidence supports this assumption. TM 266-01-050 is a left ulnar diaphysis of 239 mm long (Fig. 5, Supporting table 1, Extended data 2) showing eroded proximal epiphysis. The right ulna (TM 266-01-358) corresponds to a proximal-half shaft of 155 mm long with partially preserved epiphysis. The shafts are curved in profile. Similar anteroposterior curvature

is observed in *Ar. kadabba*[38] (ALA-VP 2/101) and later hominins StW 573k and OH 36, as in extant apes[9,39,40]. This feature contrasts with the straight right ulnar shafts of *D. guggenmosi* and *A. prometheus,* but this lack of curvature is likely due to a pathological condition[9,13]. In primates, such ulnar curvature is due to habitual loads exerted by the action of m. *brachialis* in order to maintain elbow flexion in arboreal context, which in turn involves the antagonistic action of a powerful forearm musculature, including wrist and fingers extensors and flexors[40,41].

The preserved flat distal portion of the olecranons indicate that they were not projecting posteriorly as in extant African apes[42]. In this regard, the distal portion of the olecranon most resembles the condition seen in Miocene apes[42-44] and in hominins[42]. The proximal epiphyses indicates an anteriorly-facing trochlear notch as in fossil hominins and Miocene apes[9,13,42-45]. Hence, the Toros-Menalla ulnae depart from the typical proximally oriented trochlear notch in extant great apes[41,46]. In functional terms, a more anteriorly facing notch, associated with an olecranon aligned with the long axis of the forearm, favors triceps leverage at mid-flexion[41,46]. In *Ar. ramidus* such function is linked to careful climbing and bridging[44]. Conversely, a more proximally facing notch reflects differential loading during suspension[43] while a posteriorly projecting olecranon favors triceps leverage in extension and is commonly associated with terrestrial quadrupedal locomotion in anthropoids[42].

Ulnae from Toros-Menalla display a keeled trochlear notch with a comparatively acute angle relative to later hominins and African apes. The distal keeling angle, measured from TM 266-01-358 (distal keeling angle=109°), is in the lower range of *Pongo pygmaeus* and close to the value reported for *Oreopithecus bambolii* and the left ulna AL 288-1t in *A. afarensis*[46]. Likewise, the proximal angle is acute (proximal keeling angle=100°), in the lower range of reported values for chimpanzees, and close to OH 36 and *Or. bambolii*[46]. A pronounced trochlear keel warrants medio-lateral stability of the elbow in response to powerful superficial finger and wrist flexors, and forearm pronator (*mm flexor digitorum superficialis*, *flexor carpi radialis* and *ulnaris*, and *pronator teres*)[39,46]. Such configuration was supposedly reported on *D. guggenmosi*[13] and is typical of the arboreal large apes, which integrates climbing, and/or suspension in their locomotor repertoire[46]. It is unlikely to reflect habitual terrestrial quadrupedalism. The TM 266 ulnae lack prominent flexor apparatus entheses as in orangutans, *Ar. ramidus* and later hominins. In this respect, it differs from the condition seen in Miocene apes and extant quadrupedal monkeys. Such morphology precludes the possibility of quadrupedalism and, more specifically, of knuckle-walking as primary locomotor behaviors for the Toros-Menalla hominins[45].

Overall, the trochlear notch of TM 266 ulnae present an unusual morphology as the middle portion is mediolaterally narrow relative to the distal half. This waisted aspect of the trochlear notch approaches the condition seen in ‘small’ apes (humans,

chimpanzees and bonobos) and contrasts with that of 'large' apes (orangutans and gorillas). Such configuration is interpreted as locomotor-independent and rather linked to allometry[46]. The disto-medial quadrant of TM 266-01-358 is clearly more developed than the distolateral one, an intermediate morphology between humans and chimpanzees, close to that of *D. guggenmosi*[13], *A. afarensis*, and *A. prometheus* [9,46]. A developed medial portion of the trochlear notch is an adaptation for maximum joint compression medially, a configuration which could meet mechanical requirements in various non terrestrial locomotor behaviors[13,46].

Only limited portions, proximally and distally, of TM 266-01-050 allow assessing cortical bone distribution (see Supplementary notes, Extended data 4). Proximally, the percent of cortical area is 73.4 %, measured at about 70-75 % of the estimated total lengths of the ulna (see methods). At mid-shaft, the percent of cortical area is 81.0 %, falling within the variation of Late Pleistocene hominins (80.1 % ± 6.6 in *H. sapiens* and 82.8 % ± 7.1 in neandertals)[47]. Besides, I_{max}/I_{min} and I_x/I_y are respectively 2.04/1.62 at 70-75 % level and 1.71/1.13 at midshaft. Values for the Chadian ulna fall outside the reported variation for gorillas[48] and is within the range of variation in chimpanzees for proximal I_{max}/I_{min} and proximal-midshaft I_x/I_y. Besides, TM 266-01-050 is within the range of variation of Asian non-human apes for all ratios except for the lower measured proximal I_{max}/I_{min} in *Pongo*. The geometry of TM 266-01-050 deviates from circularity in the antero-posterior direction. The cortical bone is predominantly distributed antero-posteriorly as in orangutans and to a lesser extent in chimpanzees. This condition contrasts with the one seen in gorillas, which tend to grow more bone medio-laterally. Relative medio-lateral expansion is suggested to adjust for increased vertical and medio-lateral forces that apply to the forelimb in terrestrial quadrupedal primates[45,49,50]. Besides, considering comparative data available for chimpanzees and orangutans, which tend to grow more bone antero-posteriorly[51], the Chadian ulna configuration more likely reflects bending loads associated with a wide array of arboreal locomotor modes. Yet, the TM forelimb bones lack any traits typical of suspension or knuckle walking, and exhibit a configuration better seen in apes engaged in careful climbing[44]. However, the possibility that the Chadian hominin was capable of vertical climbing cannot be dismissed given the particularly keeled trochlear notch.

The Toros-Menalla femur exhibits several hallmarks of habitual terrestrial bipedalism. Among them, a well-defined broad proto-*linea aspera,* the presence of a lateral third trochanter and associated subtrochanteric platymeria without hypotrochanteric or infero-lateral fossae, is classically associated with enhanced hip flexion-extension[16,20,52], while a particularly developed *calcar femorale* facilitates compressive loads dispelling in terrestrial bipedalism[36]. These features go with an overall cortical bone distribution pattern and cross-section geometries of the femoral shaft that suggest muscular recruitments and bone loads compatibles with habitual bipedalism. Despite some of the above-mentioned traits are suggested to be the primitive condition in hominins (proximal

platymeria or gluteal tuberosity)[17], they are part of a functional complex co-opted for bipedalism. They are routinely considered as such to infer potential bipedal terrestrial locomotion in early eastern African hominins[7,8,16,18,52,53]. The Chadian hindlimb bone conforms to the overall morphological pattern of Miocene hominin terrestrial bipeds. The forelimbs morphology rules out arboreal specialization for the Chadian material, as in *Ar. ramidus*[16] and presumably *O. tugenensis*[7]. Yet, the Chadian postcranial material displays a suite of morphological features that are consistent with substantial non-stereotypical arboreal behaviors, as suggested by ulnar shaft curvature and cross-section geometrical properties, whereas the elbow morphology is potentially indicative of careful climbing[44], and does not display any evidence of knuckle-walking.

Recently, it was suggested that the putative stem hominid *D. guggenmosi* was able to use obligate arboreal bipedalism combined to suspension as early as the late middle Miocene[13]. The authors suggested that hominin terrestrial bipedalism and great ape suspension evolved from such locomotor repertoire[13]. In the lack of evidence supporting a phylogenetic relationship between hominins and Miocene European apes, we cannot infer that hominin terrestrial bipedalism originated from middle Miocene forms in Europe as suggested by [13]. Instead, the Chadian remains described herein reassert African roots. They are the first direct evidence of an obligate terrestrial bipedalism, indistinguishable from that inferred for *O. tugenensis* and *Ar. kadabba*/*ramidus*. They suggest a precocious adaptation to bipedalism after the human-chimp dichotomy[54]. The Chadian remains suggests a conservative evolution of climbing capacities, interpreted as cautious climbing as in stem apes[54]. Hence, cautious climbing modality weakens a potential role of suspension in the emergence of the hominin clade[13].

The Toros-Menalla postcranial material also reasserts the presence of cladistic hominins in the upper Miocene of Chad, within particular environmental settings. Eastern African Miocene hominins are associated with open woodland areas with significant tree cover at ~6 Ma at Lukeino[55], and a mixture of woodland combined with wet grassland for the earliest postcranial-based bipedalism occurrence in Ethiopia at 5.2 Ma (AME-VP-1/71, *Ardipithecus kadabba*)[38,56]. At 4.4 Ma, *Ar. ramidus* most probably inhabited a ground-water-fed grassy woodland (probably a palm grove) at Aramis[57-58].

Taken as a whole, eastern-African early hominins share an arboreal component in their habitat (see [57,59] for discussion on Aramis). Environmental indicators in Toros-Menalla fossiliferous area suggest heterogeneous landscape types consisting of closed forest formations (probably riparian forests), palm grove formations, and mixed/grassland formations (from woodlands to savannas/aquatic grasslands)[5,6,60]. Therefore, the Chadian hominins were probably no exception as being reliant on arboreal cover given their potential climbing abilities. As bipeds, they were not exclusive arboreal forest dwellers, because they were able to raid in near open environments for food/water resource harvesting. The association between a polyvalent locomotion (arboreality and bipedal terrestriality), and wooded formations in mesic context during at

least ~2.5 million years suggests that the ecological niche of these early hominins was not strongly tied to the expansion of relatively dry, open areas. This niche could be depicted as opportunistic in its reliance on both terrestrial and arboreal resources.

Based on molecular data, the chimpanzee-human last common ancestor (CHCLA) is estimated to occur in Africa between 10 and 7 Ma[61,62]. Indeed, fossil representatives of the panin clade are too scarce and consists in a minimum of three Middle Pleistocene teeth from the Kapthurin formation in Kenya[63] and a chimpanzee-like proximal femoral epiphysis of unknown age from the Kikorongo crater in Uganda[64]. However, at least three taxa have been described between 10 Ma and 7 Ma in African deposits: *Samburupithecus*, from Samburu Hills, around 9.5 Ma[65], *Nakalipithecus* from Nakali, around 9,8 Ma[66] and *Chororapithecus* from the Middle Awash, around 8 Ma[62,67]. These Miocene taxa are parsimoniously assigned to stem hominines[68,69], even if *Samburupithecus* displays a particularly archaic morphology[69]. *Chororapithecus* displays derived dental affinities with *Gorilla*[67]. In light of this record and of the lack of phylogenetic resolution, the ancestral condition of positional behaviour in African apes and humans will remain elusive until significant new data becomes available. To date, the identification of the derived traits shared by hominins relies on the analysis of the earliest forms of the clade. The early hominins *Sahelanthropus, Orrorin* and *Ardipithecus* share the same combination of non-honing C-P3 complex and of features linked to terrestrial bipedalism. This combination is arguably more similar to the condition observed in later hominins than in any other African fossil or extant hominoids. This is currently the only data available for formulating scenarios about the latest Miocene/earliest Pliocene evolution of African hominoids. In absence of Mio-Pliocene fossils displaying exclusive morphological affinities with *Pan*, cautionary tales about rampant homoplasy and character polarity in this evolutionary sequence[70] are poorly suitable to falsification attempts. Instead, the morphological homogeneity of the purported hominids implies that the interpretation of the combined non-honing C-P3 complex-bipedal hindlimb as a synapomorphic signature of early hominids currently remains the most parsimonious hypothesis

References

1. Brunet, M. *et al.* A new hominid from the Upper Miocene of Chad, Central Africa. *Nature* **418**, 145-151 (2002).
2. Brunet, M. *et al.* New material of the earliest hominid from the Upper Miocene of Chad. *Nature* **434**, 752-755 (2005).
3. Vignaud, P. *et al.* Geology and palaeontology of the Upper Miocene Toros-Menalla hominid locality, Chad. *Nature* **418**, 152-155 (2002).
4. Lebatard, A. E. *et al.* Cosmogenic nuclide dating of *Sahelanthropus tchadensis* and *Australopithecus bahrelghazali*: Mio-Pliocene hominids from Chad. *Proc. Natl. Acad. Sci.*

USA **105**, 3226-3231 (2008).
5. Le Fur, S., Fara, E., Mackaye, H. T., Vignaud, P., & Brunet, M. The mammal assemblage of the hominid site TM266 (Late Miocene, Chad Basin): ecological structure and paleoenvironmental implications. *Naturwissenschaften* **96**, 565-574 (2009).
6. Schuster, M. *et al.* Chad Basin: paleoenvironments of the Sahara since the Late Miocene. *C. R. Geosci.* **341**, 603-611 (2009).
7. Senut, B. *et al.* First hominid from the Miocene (Lukeino formation, Kenya). *C. R. Acad. Sci. Paris IIA* **332**, 137-144 (2001).
8. Pickford, M., Senut, B., Gommery, D., & Treil, J. Bipedalism in *Orrorin tugenensis* revealed by its femora. *C. R. Palevol* **1**, 191-203 (2002).
9. Heaton, J. L. *et al.* The long limb bones of the StW 573 *Australopithecus* skeleton from Sterkfontein Member 2: Descriptions and proportions. *J. Hum. Evol.* **133**, 167-197 (2019).
10. Lovejoy, C. O., Cohn, M. J., & White, T. D. Morphological analysis of the mammalian postcranium: a developmental perspective. *PNAS*, **96**, 13247-13252 (1999).
11. Tardieu, C. Development of the human hind limb and its importance for the evolution of bipedalism. *Evol Anthrop: Issues, News, and Reviews*, **19**, 174-186 (2010).
12. Marchi, D. *et al.* The thigh and leg of Homo naledi. *J. Hum. Evol.* **104**, 174-204 (2017).
13. Böhme, M. *et al.* A new Miocene ape and locomotion in the ancestor of great apes and humans. *Nature*, **575**, 489-493 (2019).
14. Ruff, C. in *Primate Locomotion: Recent Advances* (eds. Strasser, E., Fleagle, J., Rosenberger, A.L., & McHenry, H.) 449-469 (Springer, Boston, MA, 1998).
15. Lovejoy, C. O., Meindl, R. S., Ohman, J. C., Heiple, K. G., & White, T. D. The Maka femur and its bearing on the antiquity of human walking: applying contemporary concepts of morphogenesis to the human fossil record. *Am. J. Phys. Anthropol.* **119**, 97-133 (2002).
16. Lovejoy, C. O., Suwa, G., Spurlock, L., Asfaw, B., & White, T. D. The pelvis and femur of *Ardipithecus ramidus*: the emergence of upright walking. *Science* **326**, 71e1-71e6 (2009).
17. Almécija, S. *et al.* The femur of *Orrorin tugenensis* exhibits morphometric affinities with both Miocene apes and later hominins. *Nat. Commun.* **4**, 2888 (2013).
18. Richmond, B. G., & Jungers, W. L. *Orrorin tugenensis* femoral morphology and the evolution of hominin bipedalism. *Science* **319**, 1662-1665 (2008).
19. Pina, M. *Unravelling the positional behaviour of fossil hominoids morphofunctional and structural analysis of the primate hindlimb*. Doctoral dissertation, Universitat Autònoma de Barcelona (2016).
20. Morimoto, N., De León, M. S. P., Nishimura, T., & Zollikofer, C. P. Femoral morphology and femoropelvic musculoskeletal anatomy of humans and great apes: a comparative virtopsy study. *Anat. Rec.* **294**, 1433-1445 (2011).

21. Macchiarelli, R. & Zanolli, C. Hominin biomechanics, virtual anatomy and inner structural morphology: From head to toe. A tribute to Laurent Puymerail. *C. R. Palevol* **16**, 493–498 (2017).
22. Eckhardt, R. B., Galik, G., & Kuperavage, A. J. Questions about *Orrorin* femur: response. *Science* **307**, 845 (2005).
23. Galik, K. *et al.* External and internal morphology of the BAR 1002'00 *Orrorin tugenensis* femur. *Science* ***305***, 1450-1453 (2004).
24. Ohman, J. C., Lovejoy, C. O., & White, T. D. Questions about *Orrorin* femur. *Science* **307**, 845 (2005).
25. Lieberman, D. E., Polk, J. D., & Demes, B. Predicting long bone loading from cross□ sectional geometry. *Am. J. Phys. Anthropol.* **123***,* 156-171 (2004).
26. Ruff, C. B., Burgess, M. L., Ketcham, R. A., & Kappelman, J. Limb Bone Structural Proportions and Locomotor Behavior in AL 288-1 (" Lucy"). *PLoS ONE* **11**, e0166095 (2016).
27. Lovejoy, C. O., Burstein, A. H., & Heiple, K. G. The biomechanical analysis of bone strength: a method and its application to platycnemia. *Am. J. Phys. Anthropol.* **44**, 489-505 (1976).
28. Mongle, C. S., Wallace, I. J. & Grine, F. E. Cross-sectional structural variation relative to midshaft along hominine diaphyses. II. The hind limb. *Am. J. Phys. Anthropol.* **158**, 398- 407 (2015).
29. Trinkaus, E. & Ruff, C. B. Femoral and Tibial Diaphyseal Cross-Sectional Geometry in Pleistocene *Homo*. *PaleoAnthropology* **2012**, 13-62 (2012).
30. Nadell, J. *Ontogeny and Adaptation: A Cross-Sectional Study of Primate Limb Elements*. Doctoral dissertation, Durham University (2017).
31. Puymerail, L. *et al.* Structural analysis of the Kresna 11 *Homo erectus* femoral shaft (Sangiran, Java). *J. Hum. Evol.* **63**, 741-749 (2012).
32. Ruff, C. Femoral/humeral strength in early African *Homo erectus*. *J. Hum. Evol.* **54**, 383-390 (2008).
33. Ruff, C. Relative limb strength and locomotion in *Homo habilis*. *Am. J. Phys. Anthropol.* **138**, 90-100 (2009).
34. Ruff, C. B., Puymerail, L., Macchiarelli, R., Sipla, J., & Ciochon, R. L. Structure and composition of the Trinil femora: functional and taxonomic implications. *J. Hum. Evol.* **80**, 147-158 (2015).
35. Chevalier, T. AL 333-61 femoral diaphysis: evidence of obligate bipedalism 3.2 million years ago in Ethiopia? *Bull. Mém. Soc. Anthropol. Paris* **25**:169-189 (2013).
36. Kuperavage, A., Pokrajac, D., Chavanaves, S. & Eckhardt, R. B. Earliest known hominin *calcar femorale* in *Orrorin tugenensis* provides further internal anatomical evidence for origin of human bipedal locomotion. *Anat. Rec.* **301**, 1834-1839 (2018).
37. Zhang, Q. *et al*. The role of the *calcar femorale* in stress distribution in the proximal femur. *Orthop. surg.*, **1**, 311-316 (2009).

399 38. Haile-Selassie, Y., Suwa, G. & White, T. in *Ardipithecus kadabba: Late Miocene*
400 *Evidence From The Middle Awash, Ethiopia* (eds. Haile-Selassie, Y., & WoldeGabriel,
401 G.) 159-236 (Univ of California Press, 2009).
402 39. Drapeau, M. S. M., Ward, C. V., Kimbel, W. H., Johanson, D. C., & Rak, Y.
403 Associated cranial and forelimb remains attributed to *Australopithecus afarensis* from
404 Hadar, Ethiopia. *J. Hum. Evol.* **48**, 593-642 (2005).
405 40. Henderson, K., Pantinople, J., McCabe, K., Richards, H. L. & Milne, N. Forelimb
406 bone curvature in terrestrial and arboreal mammals. *PeerJ* **5**, e3229 (2017).
407 41. Drapeau, M. S. M. Functional anatomy of the olecranon process in hominoids and
408 Plio-Pleistocene hominins. *Am. J. Phys. Anthropol.* **124**, 297-314 (2004).
409 42. Begun, D. R. Phyletic diversity and locomotion in primitive European hominids. *Am.*
410 *J. Phys. Anthropol.* **87**, 311-340 (1992).
411 43. Takano, T. *et al.* Forelimb long bones of *Nacholapithecus* (KNM-BG 35250) from the
412 middle Miocene in Nachola, northern Kenya. *Anthropol. Sci.* **126**, 135-149 (2018).
413 44. Lovejoy, C. O., Simpson, S. W., White, T. D., Asfaw, B., & Suwa, G. Careful climbing
414 in the Miocene: the forelimbs of *Ardipithecus ramidus* and humans are primitive. *Science*
415 **326**, 70e1-70e8 (2009).
416 45. Alba, D. M., Almécija, S., Casanovas-Vilar, I., Méndez, J. M., & Moyà-Solà, S. A
417 partial skeleton of the fossil great ape *Hispanopithecus laietanus* from Can Feu and the
418 mosaic evolution of crown-hominoid positional behaviors. *PLoS ONE* **7**, e39617 (2012).
419 46. Drapeau, M. S. M. Articular morphology of the proximal ulna in extant and fossil
420 hominoids and hominins. *J. Hum. Evol.* **55**, 86-102 (2008).
421 47. Churchill, S. E. *et al.* Morphological affinities of the proximal ulna from Klasies River
422 main site: archaic or modern? *J. Hum. Evol.* 31, 213-237 (1996).
423 48. Nadell, J.A. Ontogeny and adaptation: a cross-sectional study of primate limb
424 elements, Doctoral dissertation, Durham University (2017).
425 49. Carlson, K.J. et al. Role of nonbehavioral factors in adjusting long bone diaphyseal
426 structure in free-ranging Pan troglodytes. *Int. J. Primatol*. **29**, 1401-1420 (2008).
427 50. Schmitt, D. Mediolateral reaction forces and forelimb anatomy in quadrupedal
428 primates: implications for interpreting locomotor behavior in fossil primates. *J. Hum.*
429 *Evol.* **44**, 47-58 (2003).
430 51. Morimoto, N. *et al.* Let bone and muscle talk together: a study of real and virtual
431 dissection and its implications for femoral musculoskeletal structure of chimpanzees. *J.*
432 *Anat.* **226**, 258-267 (2015).
433 52. White, T. D. *et al.* Asa Issie, Aramis and the origin of *Australopithecus*. *Nature* **440**,
434 883-889 (2006).
435 53. Ward, C. V., Kimbel, W. H., Harmon, E. H. & Johanson, D. C. New postcranial
436 fossils of *Australopithecus afarensis* from Hadar, Ethiopia (1990–2007). *J. Hum. Evol.*
437 **63**, 1-51 (2012).
438 54. Lovejoy, C. O. et al. The great divides: Ardipithecus ramidus reveals the postcrania

of our last common ancestors with African apes. *Science* **326**, 73-106 (2009).
55. Bamford, M. K., Senut, B. & Pickford, M. Fossil leaves from Lukeino, a 6-million-year-old Formation in the Baringo Basin, Kenya. *Geobios* **46**, 253-272 (2013).
56. WoldeGabriel, G. et al. Geology and palaeontology of the late Miocene Middle Awash valley, Afar rift, Ethiopia. *Nature* **412**, 175-178 (2001).
57. White, T. D. *et al.* Macrovertebrate paleontology and the Pliocene habitat of *Ardipithecus ramidus*. *Science* **326**, 67-93 (2009).
58. Barboni, D., Ashley, G. M., Bourel, B., Arraiz, H. & Mazur, J. C. Springs, palm groves, and the record of early hominins in Africa. *Rev. Palaeobot. Palynol*. **266**, 23-41 (2019).
59. Cerling, T. E. *et al.* Woody cover and hominin environments in the past 6 million years. *Nature* **476**, 51-56 (2011).
60. Novello, A. *et al.* Phytoliths indicate significant arboreal cover at *Sahelanthropus* type locality TM266 in northern Chad and a decrease in later sites. *J. Hum. Evol.* **106**, 66-83 (2017).
61. Steiper, M. E. & Young, N. M. Timing primate evolution: lessons from the discordance between molecular and paleontological estimates. *Evol. Anthropol.* **17**, 179-188 (2008).
62. Katoh, S. *et al*. New geological and palaeontological age constraint for the gorilla–human lineage split. *Nature* **530,** 215-218 (2016).
63. McBrearty, S. & Jablonski, N. G. First fossil chimpanzee. *Nature* ***437***, 105-108 (2005).
64. DeSilva, J., Shoreman, E. & MacLatchy, L. A fossil hominoid proximal femur from Kikorongo Crater, southwestern Uganda. *J. Hum. Evol.* ***50***, 687-695 (2006).
65. Ishida H. & Pickford M. A new late Miocene hominoid from Kenya: *Samburupithecus kiptalami gen.* et sp. nov. *C.R. Acad. Sci. Paris* **325**,823–829 (1997).
66. Kunimatsu, Y. et al. A new Late Miocene great ape from Kenya and its implications for the origins of African great apes and humans. Proc. Natl Acad. Sci. USA **104**, 19220-19225 (2007).
67. Suwa G., Kono R.T., Katoh S., Asfaw B. & Beyene Y. A new species of great ape from the late Miocene epoch in Ethiopia. *Nature* **448**, 921–924 (2007).
68. Harrison, T. in Cenozoic Mammals of Africa (eds. Werdelin, L. & Sanders,W.J.) 429-469 (Univ of California Press, Berkeley, 2010).
69. Begun, D.R. in Handbook of Paleoanthropology, (eds. Henke, W. & Tattersall, I.) 1261 - 1332 (Springer-Verlag, Berlin Heidelberg, 2015)
70. Wood, B. & Harrison, T. The evolutionary context of the first hominins. *Nature* **470**: 347-352 (2011).

Methods

The original fossil specimens are measured to the nearest 0.1 mm using a Mitutoyo

sliding digital caliper.

Computed tomography

High-resolution micro-computed tomography (HR-mCT) images taken from the original femur and ulnae were used to assess the inner morphology of the bones. The material was scanned with EasyTom XL Duo mCT (using a sealed Hamamatsu microfocus x-ray source - 75 W, 150 kV - and an amorphous silicon based detector Varian PaxScan 2520DX, 1536*1920 pixel matrix; 127 mm pixel pitch, 16 bits, CsI conversion screen - from RX-Solutions, France) at Plateforme PLATINA (University of Poitiers). For scanning procedures, beam intensity was set at 90 kV and tube current at 333 mA. The TM 266- 01-358 ulna was acquired with 3584 projections resulting in 3036 slices of 730*825 pixels using a cone-beam reconstruction algorithm. The isovoxel size was set to 0.0525 mm. The TM 266-01-050 ulna was acquired with 4800 projections resulting in 4051 slices of 589*849 pixels. The isovoxel size was set to 0.0600 mm. The TM 266-01-063 femur was acquired with 5984 projections resulting in 4962 slices of 1162*911 pixels. The isovoxel size was set to 0.0499 mm.

Virtual models processing

Semi-automatic segmentation of the virtual fossil specimens and three-dimensional surfaces extraction were performed in Avizo Lite. Three-dimensional surfaces were prepared and treated using Geomagic Studio. Cortical bone thickness distribution was assessed in three dimensions using the *Surface thickness* module in Avizo Lite from the outer surface of the of the segmented medullar cavity to the outer surface of the femur. All measurements based on 3D virtual models of the fossil specimen were done in Avizo Lite on 3D volumes and Fiji image software[71] on 2D slices.

Cross-sectional geometric properties (CSGP)

The femur lacks the most part of the epiphyses, which prevents from estimating its biomechanical length. However, CSGP values in *Homo* and *Pan* do no show significant differences between 45-55 % of the femoral (biomechanical or maximum) length[31]. Comparison of diaphyseal cross-sectional geometry from fragmentary specimens must be evaluated on a case-by-case basis[31]. Superimposition of the femora BAR 1002'00 (*O. tugenensis*) and TM 266-01-063 using the distal base of their lesser trochanter (corresponding to 80 % of the biomechanical length[72]), show that the nutrient foramen on TM 266-01-063 provides a reliable indicator of the midshaft level. CSGP estimates were computed at nutrient foramen level and then, in order to get an assessment of the variation pattern of cortical bone distribution, at four additional cross-sections, equally spaced from the nutrient foramen to the base of the lesser trochanter. For ulnae, CSGP variables were computed proximally from 35.0 mm below the distal border of the radial notch (and at the level of the nutrient foramen), which corresponds to 70-75 % of the estimated ulna length for TM 266-01-050 (estimated using OMO L40-19 fossil hominin ulna as analog).

519 Percentage of cortical area and second moment of area were computed using Fiji
520 image software[71] and BoneJ plugin[73].
521 Comparative data for CSGP with extant and extinct hominoids (Extended data 4)
522 were gathered from [19,21,26,28-30,32,33,35,74,75].
523
524 71. Schindelin, J. et al. Fiji: an open-source platform for biological-image analysis.
525 Nature methods **9**, 676-682 (2012).
526 72. Ruff, C. B. Long bone articular and diaphyseal structure in Old World monkeys and
527 apes. I: locomotor effects. *Am. J. Phys. Anthrop.* **119**, 305-342 (2002)
528 73. Doube, M. *et al.* BoneJ: Free and extensible bone image analysis in ImageJ. *Bone*
529 **47**, 1076-1079 (2010).
530 74. MaClatchy, L., Gebo, D., Kityo, R., & Pilbeam, D. Postcranial functional morphology
531 of *Morotopithecus bishopi*, with implications for the evolution of modern ape locomotion.
532 *J. Hum. Evol.* **39**, 159-183 (2000).
533 75. Rodríguez, L., Carretero, J. M., García-González, R., & Arsuaga, J. L. Cross-
534 sectional properties of the lower limb long bones in the Middle Pleistocene Sima de los
535 Huesos sample (Sierra de Atapuerca, Spain). *J. Hum. Evol.* **117**, 1-12 (2018).
536
537 **Acknowledgments** We thank the Chadian Authorities (Ministère de l'Education
538 Nationale de l'Enseignement Supérieur, de la Recherche et de l'Innovation, Université
539 de Djamena & CNRD). We extend gratitude for their support to the French Ministries,
540 Ministère Français de l'Education Nationale (Collège de France, Université de Poitiers),
541 Ministère de la Recherche (CNRS), Ministère de l'Europe et des affaires étrangères
542 (Direction de la Coopération Scientifique, Universitaire et de Recherche, Paris, and
543 SCAC Ambassade de France à N'djamena, Commission de Consultation des
544 recherches Archéologiques à l'Etranger), to the Région Nouvelle Aquitaine, and also to
545 the Armée Française (MAM, Epervier and Barkhane) for logistic support. We would like
546 to thank deeply to Professor M. Brunet, head of the M.P.F.T., who initiated this work and
547 gathered the first comparative data at the basis of the present manuscript. For giving him
548 the opportunity to work with their collections, we are grateful to our Colleagues and their
549 Institutions: C.O. Lovejoy (Kent State University), B. Asfaw (National Museum of
550 Ethiopia), Y. Haile-Selassie (Cleveland Museum of Natural History), M. G. Leakey & R.
551 Leakey (National Museum of Kenya), D. Pilbeam (Peabody Museum and Harvard
552 University), D. Johanson & W. Kimbel (Institute of Human Origins and Arizona State
553 University at Tempe), T. White (University of California at Berkeley) and G. Suwa
554 (University Museum of Tokyo). Special thanks to all our colleagues and friends for their
555 help and discussion, and particularly to D. Barboni, A. Mazurier (Centre de
556 Microtomographie), A. Novello. We especially thank all the MPFT members who
557 participated to the field missions, and Ahounta D., Fanoné G. (deceased), Mahamat A.,
558 S. Riffaut, J. Surault and X. Valentin for technical support. We are most grateful to G.

Florent, C. Noël, G. Reynaud, C. Baron, M. Pourade, and L. Painault for administrative guidance.

Author contributions

G.D. and F. G. designed the study, collected and interpreted the data. G.D., F.G. and J.-R. B. wrote the manuscript. G. D., F. G., J.-R. B., M.H.T., A.L., M.A., P.V. and C.N. discussed the results and revised earlier drafts of the papers.

Figure legends

Fig.1 | Femoral remain of *S. tchadensis* from late Miocene at Toros-Menalla 266th locality. Virtual representation of TM 266-01-063: a, anterior view; b, posterior view; c, medial view; d, lateral view; e, enlarged view of the proximal portion: e, lateral view; g, anterior view; microCT-slices at the level of the third trochanter (f); microCT-slices of the distal part of the femoral neck (g, h). The asterisks mark the microCT-slice levels and orientations.

Fig.2 | Cross-sectional geometric properties of the TM 266-01-063 femur. a, microCT-slice levels and corresponding percent of cortical area; b, microCT-slice images; c, interpretive drawings of the cortical thickness at microCT-slice levels, numbers are for the measured cortical thickness anteriorly, posteriorly, medially and laterally (in mm), maximum thickness is in red while minimum thickness is in green. TA, total area in mm^2; CA, cortical area in mm^2; %, percent of cortical area.

Fig.3 | Three-dimensional cortical thickness of TM 266-01-063. a, anterior view; b, posterior view; c, medial view; d; lateral view. Scale bar is 20 mm. Chromatic scale corresponds to the look-up table of cortical thickness (in mm).

Fig.4 | Illustration of the TM 266-01-063 *calcar femorale*. a, virtual representation of the proximal portion of the femur, posterior view; b, microCT-slice at the lesser trochanter level showing proximo-distal extension of the *calcar femorale* (asterisk); c, virtual representation of the proximal portion of the femur showing microCT-slice levels and orientations; d, e, f, g, h, microCT-slice images for respectively slice levels from 1 to 5, showing expression of the *calcar femorale* transversally.

Fig.5 | Ulnar remains of *S. tchadensis* from Late Miocene at Toros-Menalla 266 locality. TM 266-01-358: a, anterior view; b, posterior view; c, medial view; d, lateral

view. TM 266-01-050: e, anterior view; f, posterior view; g, lateral view; h, medial view. MicroCT-slices images levels and orientations are numbered from 1 to 3 and i to iv respectively. The asterisks mark the location of the nutrient foramina.

Extended data

Extended data 1. Schematic Map of the Repblic of Chad and localization of TM 266 locality.

Extended data 2. Illustration of the postcranial original material from Toros-Menalla, Chad. TM 266-01-063 femur: a, anterior view; b, posterior view; c, lateral view; d, medial view. TM 266-01-358 ulna: e, anterior view; f, posterior view; g, lateral view; h, medial view. TM 266- 01-050 ulna: i, anterior view; j, posterior view; k, lateral view; l, medial view.

Extended data 3. Illustration and estimation of the femoral anteversion. a. view of the femur showing proximal plan; b view of the femur showing the distal plan; c, micro-CT slice showing the major axis of the diaphyseal proximal cross section; d, micro-CT slice showing the major axis of the diaphyseal distal cross section; e, superimposition of the medial and distal axes forming an angle of about 26°.

Extended data 4. Comparative CSGP data for TM 266 femur and ulnae. Comparisons of the TM 266-01-50 ulna and extant hominoid values for a, I_{max}/I_{min} and b, I_x/I_y. Comparisons of the TM 266-01-063 femur and extant hominoid values for c, I_{max}/I_{min}; d, I_x/I_y and e, %CA (see methods). Circles are for means and whiskers for standard deviations.

Supplementary Information

1. Supplementary Table

Supplementary Table 1. Morphological state of the main preserved features in *S. tchadensis* femur and ulnae and their comparative in the extant and extinct homininae.

2. Supplementary Notes

1. Detailed descriptions of the TM 266 hominin postcranial material

Left femur (TM 266-01-063)

TM 266-01-063 is a left femoral shaft of about 242 mm, lacking the distal epiphysis and its adjoining metaphyseal region, and most of the proximal epiphysis. The femoral shaft is curved antero-posteriorly. The femoral head is missing, the neck being broken about 15 mm above the margin, which delineates the lesser trochanter proximally. In proximal view, the neck is compressed antero-posteriorly. The medial border of the neck is oriented proximally, only the medialmost portion of the intertrochanteric line is visible. Lateral to the neck, the greater trochanter and the trochanteric fossa are lacking. The preserved portion of the posterior face of the neck presents a slight depression, which could be evidence of the presence of the *externus obturator*. The lesser trochanter preserves only its basal surface bordered by a prominent margin. It has a raindrop shape, of 25.3 mm long and 16.2 mm wide. Preserved evidences suggest that the lesser trochanter was substantially developed albeit there is no definitive indication on its overall orientation. The lesser trochanter connects to the neck with a slightly concave surface. There is no evidence of an intertrochanteric crest. A linea pectinea, expressed by a bulge, arise from the distal margin that delineates the lesser trochanter. There is no evidence of a hypotrochanteric fossa or lateral pilaster. There is no evidence of superomedial and inferolateral fossae. Just distal to the lesser trochanter location, the diameter of the shaft is 24.0 mm antero-posteriorly and 32.0 mm medio-laterally illustrating subtrochanteric platymery.

Lateral to the lesser trochanter level, the insertion of the *gluteus maximus* left a small but sharp relief, indicative of the third trochanter, continuing into a rugose surface distally. This rugose surface blends with the lateral component of the *linea aspera* distally. Medially to the lesser trochanter runs the spirale line for the insertion of the *vastus medialis*. It consists in a straight line, which confounds distally with the medial border of the spirale line. The linea spirale delimits posteriorly a medial shallow fossa.

The lateral border of the *linea aspera* forms a well-marked, sigmoid, and continuous line from the gluteal ridge to approximately 37.5 mm to the distalmost end of the shaft. It curves medially at about 20 mm distal to the nutrient foramen. The medial and lateral borders of the *linea aspera* do not form a pilaster. The distance between medial and lateral borders of the *linea aspera* is 12.2 mm in its minimum. The anterior face of the proximal end bears a large slightly concave surface, with no discernable relief except a restricted rugose surface located on the proximal border. There is no evidence of the femoral tubercle.

Enlargement of the diaphysis start soon after mid-shaft. Distally, there is no anatomical evidence to estimate the location of the metaphyseal region. The medial and lateral borders of the *linea aspera* diverge at about the distal fifth of the shaft length. In anterior view, no patellar fossa is visible. No reliable indicator allows estimating the length of the missing distal portion of the femur.

Inner structure: The medullar cavity is almost completely filled by sediment and no trabecular network is preserved except at proximal end with limited evidences close to the cortical bone. At this level, the lesser trochanter is strengthened internally by a spur of bone, also called *calcar femorale*, projecting out superiorly from the cortex into central cancellous bone. Precise location of the midshaft is uncertain, but there is a distinct nutrient foramen located posteriorly at about the maximum of curvature of the shaft. Overall preservation of the bone and taphonomic aspects prevents from having exact estimation of the average cortical thickness. Nevertheless, linear measurements obtained from micro-CT slice orthogonal to the long axis of the shaft, at nutrient foramen show thickest cortical bone laterally and thinnest anteriorly. The outline of the bone at the same level of the shaft is subcircular with a posterior flattened portion corresponding to the space between the lateral and medial margins of the *linea aspera* (diameters are 27.6 mm mediolaterally and 25.3 mm anteroposteriorly).

***Right ulna* (TM 266-01-358)**

It is a half proximal portion of a right ulna, of about 155 mm, preserving most of the proximal epiphysis. The trochlear notch is almost complete but the anteroproximal end of the anconeal process and most part of the posteroproximal portion of the olecranon. At the level of the coronoid process, the preserved posterior portion of the ulna suggests olecranon does not project posteriorly. The trochlear notch is keeled, narrow in its middle portion, and enlarging distally. In anterior view, the trochlear notch axis defined by the anconeal and coronoid processes is in line with shaft axis. In medial/lateral view, the trochlear notch faces anteriorly. The distomedial portion of the trochlear notch is weakly concave and is proportionally large mediolaterally when compared with its lateral counterpart.

The articular surface of the radial notch is not preserved but its outline shows that it was not rounded but rather subrectangular with 16.2 mm wide anteroposteriorly and 12.6 mm long proximodistally. The radial notch is on a promontory. In proximal view, the plan of the radial notch makes an acute angle (~30°) with the major axis (as defined by the keeling axis) of the trochlear notch. In the coronal plan, the radial notch should have not been vertical but slightly oblique distally. Distally, the supinator crest emerges directly from the posterior border of the radial notch and run distally for about 40 mm, the distal end being difficult to estimate due to taphonomic alterations.

Posteriorly to the supinator crest, a wide and concave fossa for the *anconeus* is posteriorly delimited by a sharp crest running from the base of the olecranon process to 15 mm distally to the level of the distal border of the radial fossa and then become smooth. Distally, the shaft is subtriangular in section. It is defined by an anterior edge due to the insertion of the interosseous membrane, this later separates medially the face for the *flexor digitorum profondus*, and laterally the face for the *extensor ulnaris carpi*.

The posterior border is delimited laterally by the crest delimiting the *anconeus* attachment and medially by the edge for the insertion of the *flexor ulnaris carpi*. The proximal portion dedicated for the attachment of the *flexor digitorum profundus* corresponds to a large and shallow depression. The shaft is curved in profile and twists transversally, the insertion of the interosseous membrane deviating laterally.

Left ulna **(TM 266-01-050)**

TM 266-01-050 consists in a left ulnar diaphysis of 239 mm long as preserved. The proximal epiphysis is badly damaged. In anterior view, the trochlear notch is eroded preserving only a small distal portion of the *anconeus* process. Most part of the olecranon is missing but its preserved posterodistal portion indicates olecranon does not project posteriorly.

In overall shape, the trochlear notch is narrow in its middle portion. The coronoid process is unpreserved, making impossible any reliable estimation of the trochlear notch angle. The fossa for the *brachialis* is located anteriorly, in line with the estimated trochlear notch axis (as defined by the anconeal-coronoid processes) and is 15-16 mm long.

The articular surface of the radial notch is lacking. The radial notch is on a promontory which outline is comparable in shape to the right ulna. Distally, the supinator crest emerges directly from the posterior border of the radial notch, and despite taphonomic damage shows comparable condition to the right ulna.

Posteriorly to the supinator crest, a wide and concave fossa for the *anconeus* is posteriorly delimited by a sharp crest running distally from the base of the olecranon process to the level of the radial fossa and then fades into a rounded margin. At midshaft, the ulna is subtriangular in section, in the same configuration of the right ulna and becomes oval distally. As for TM 266-01-358, the posterior face of the ulna is bordered laterally by the crest delimiting the *anconeus* attachment and medially by the insertion edge for the *flexor ulnaris carpi*, forming a noticeable flat surface. The proximal portion dedicated for the attachment of the *flexor digitorum profundus* corresponds to a large and shallow depression. There is no medial protuberance for the attachment of the *flexor digitorum profundus*. The shaft is curved in profile, sigmoid coronally and twists transversally, the insertion of the interosseous membrane deviating laterally. Distally, the shaft is likely broken proximal to the quadratus pronator attachment.

The nutrient foramen is located at 92 mm from the anteroproximal surface of the lateral quadrant of the trochlear notch.

2.2. Context of the discoveries

The Mission Paléontologique Franco-Tchadienne (MPFT, directed by Michel Brunet) has conducted field missions in the Djurab desert since 1994. Its first major discovery was a partial mandible attributed to a new species, *Australopithecus bahrelghazali*[1,2], found in the fossiliferous sector of Koro Toro (upper Pliocene). In 1997, Brunet led an exploratory team in the western part of the Djurab and discovered a new fossiliferous sector dominated by upper Miocene outcrops (Toros-Menalla, TM). From 1997 to 2001, the MPFT documented the full extension of this large area (ca. 100 km along an East-West axis) and initiated its systematic survey. In July 2001, a technical team of four MPFT members[1] performed a recognition survey at TM and reached a particularly rich area (locality TM 266), at that time a ca. 1.5 km^2 surface more or less clear of sand accumulations. The team collected an abundant sample of fossil specimens and documented photographically the work, but did not performed precise recording of specimen positions relative to each other within the locality. The partial cranium TM 266-01-060-1 proposed as holotype specimen for *Sahelanthropus tchadensis* by [3], the femur TM 266-01-063 and one of the ulnae (TM 266-01-050) were among the collected specimens. The participants to this mission reported conflicting information regarding the precise locations within the locality TM 266 of the various fossil remains collected during this mission. Pictures used to discuss the original position of the femur and cranium[4] do not include the ulna TM 266-01-050, and do not present contextual elements allowing identifying the location and timing of their shooting. Most specimens observed on these pictures, also including various craniodental and postcranial remains of other vertebrates, do not display the dust and sand coverage usually observed on surface finds in the Djurab desert: they were therefore photographed after handling. This corroborates claims by Chadian team members that these pictures did not record the initial position of the fossils and that they were shot after the fossils were gathered from the surroundings. Given the minimum number of hominin individuals calculated for TM 266 (six, among which three adults[5]), suggestions that TM 266-01-060-1 and any of the newly described postcranial elements belong to the same individual remain highly hypothetical.

In Ndjamena, the team roughly sorted the 561 specimens collected during the mission (141 for TM 266) by high-level taxonomic ranks and eventually stored most of the postcranial specimens as an “indet.” group. This was the case for the femur TM 266-01-063 and the ulna TM 266-01-050. The material then waited for examination by skilled anatomists, which did not happen during the two following years. At the time, the MPFT gave the highest priority to other tasks. First, the study of the craniodental material and the initial characterization of the TM 266 faunal assemblage occupied all the research time and resulted in their first description in Nature a year after TM 266 discovery[6,7]. Second, several field missions aimed at unearthing further specimens at TM 266 and adjacent areas in the context of quickly increasing cover of the hominin locality by eolian sands and of extreme sand-blast erosion of surface specimens. From 2001 to 2003,

despite the low density of fossil remains in Djurab fossil-bearing localities, the MPFT collected more than 7,000 specimens at TM, including new craniodental specimens attributed to *Sahelanthropus* and described by [5].

In early 2004, prior to careful examination by skilled paleontologists, various postcranial remains discovered in July 2001 were selected for the training of a master student in taphonomy, including TM 266-01-063. Seeking an identification, the student handed this specimen to Roberto Macchiarelli[8], not a member of the MPFT. Macchiarelli correctly identified the femur to be that of a hominin[8]. In parallel, the MPFT identified the ulnar remains. Later, the existence of a hominin femur from TM 266 leaked to the public prior to its formal description, damaging the ability of the MPFT to preserve the novelty of its disclosure for a formal scientific publication. Since 2004, the MPFT attempted discovering further remains documenting the postcranial anatomy of the TM hominins, to date unsuccessfully.

[1] Including three Chadian technicians of the Centre National d'Appui à la Recherche (CNAR, now CNRD) led by one “cooperation assistant” from the Embassy of France to Chad.

References

1. Brunet, M. et al. The first australopithecine 2,500 kilometres west of the Rift Valley (Chad). *Nature* **378**, 273-275 (1995).
2. Brunet et al. Beauvilain, A., Coppens, Y., Heintz, E., & Moutaye, A. E. (1996). *Australopithecus bahrelghazali*, une nouvelle espèce d'Hominidé ancien de la région de Koro Toro (Tchad). *C. R. Acad. Sci.* Paris **322**, 907-913 (1996).
3. Brunet, M. *et al.* A new hominid from the Upper Miocene of Chad, Central Africa. *Nature* **418**, 145-151 (2002).
4. Beauvilain, A., Watté, J. P. Toumaï (*Sahelanthropus tchadensis*) a t-il été inhumé ? *Bull. Soc. Géol. Normandie* **96**, 19-26 (2009).
5. Brunet, M. *et al.* New material of the earliest hominid from the Upper Miocene of Chad. *Nature* **434**, 752-755 (2005).
6. Brunet, M. *et al.* A new hominid from the Upper Miocene of Chad, Central Africa. *Nature* **418**, 145-151 (2002).
7. Vignaud, P. *et al.* Geology and palaeontology of the Upper Miocene Toros-Menalla hominid locality, Chad. *Nature* **418**, 152-155 (2002).
8. Callaway, E. Femur findings remain a secret. *Nature* **553**, 391-392 (2018).

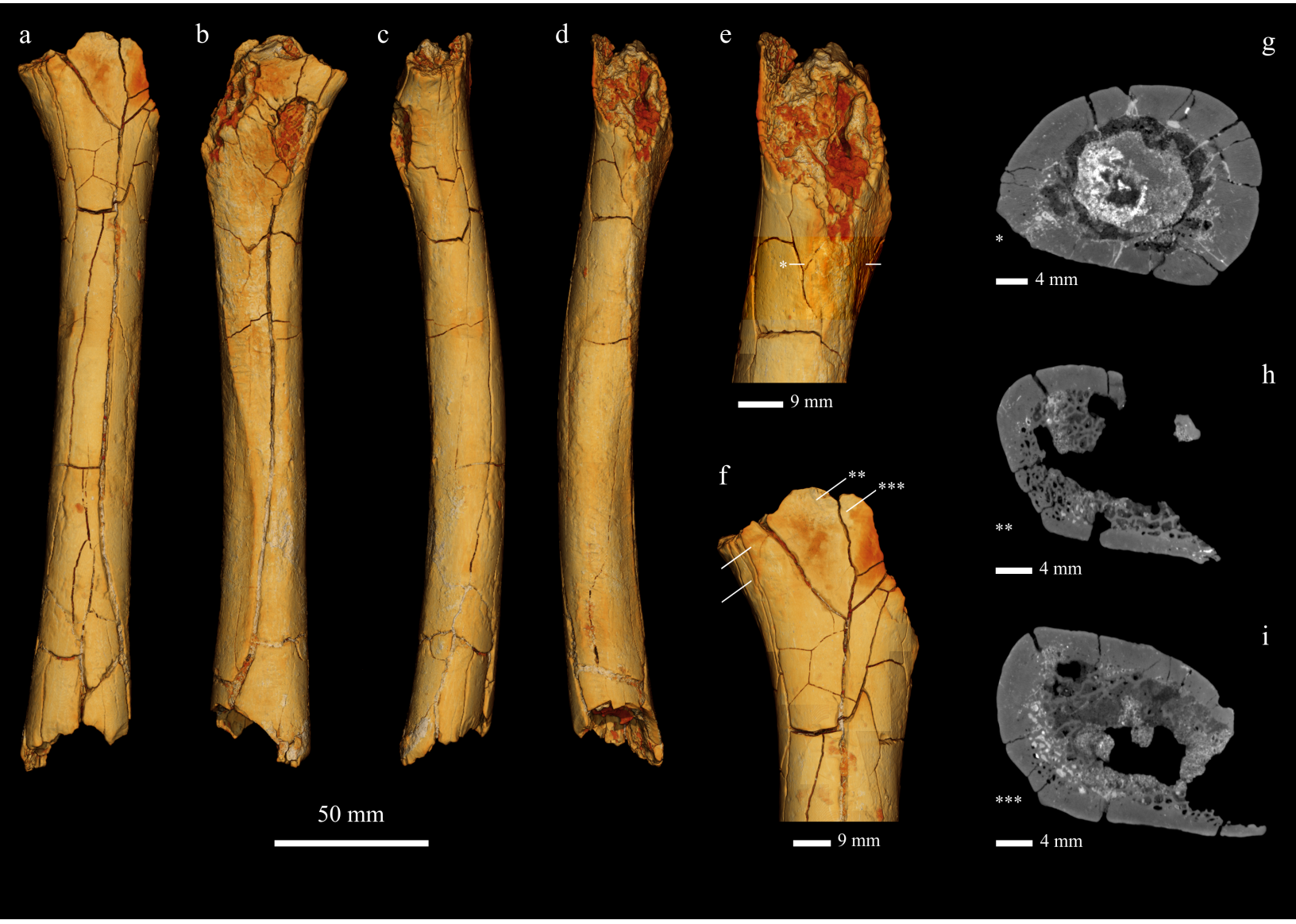
a
b
c
d
e
g
50 mm
*
4 mm
9 mm
h
f
**
***
**
4 mm
i
9 mm
***
4 mm

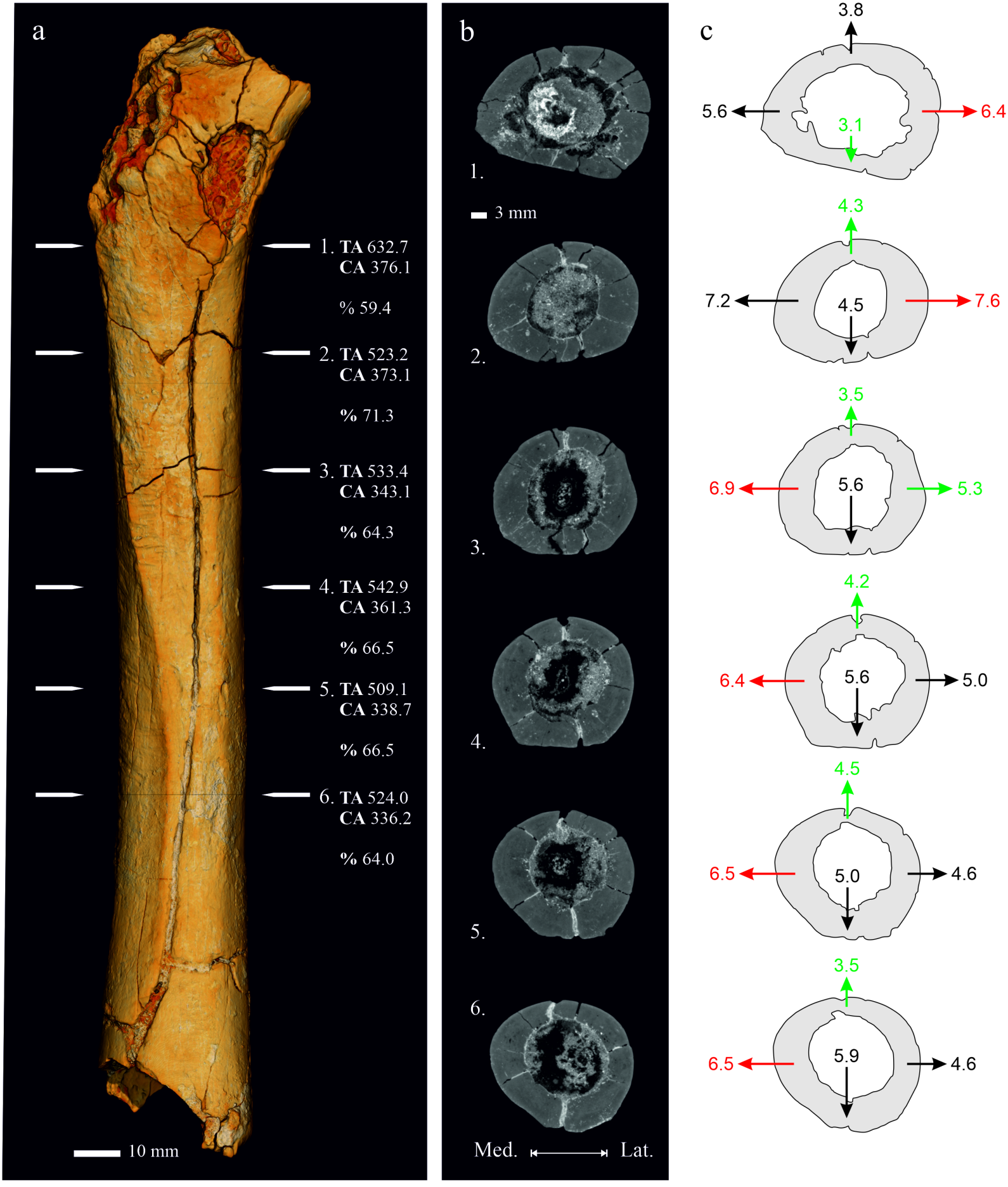
a
1. TA 632.7
CA 376.1
% 59.4
2. TA 523.2
CA 373.1
% 71.3
3. TA 533.4
CA 343.1
% 64.3
4. TA 542.9
CA 361.3
% 66.5
5. TA 509.1
CA 338.7
% 66.5
6. TA 524.0
CA 336.2
% 64.0
10 mm
b
1.
3 mm
2.
3.
4.
5.
6.
Med.
Lat.
c
3.8
5.6
3.1
6.4
4.3
7.2
4.5
7.6
3.5
6.9
5.6
5.3
4.2
6.4
5.6
5.0
4.5
6.5
5.0
4.6
3.5
6.5
5.9
4.6


a
b
c
d
Thick
Thin

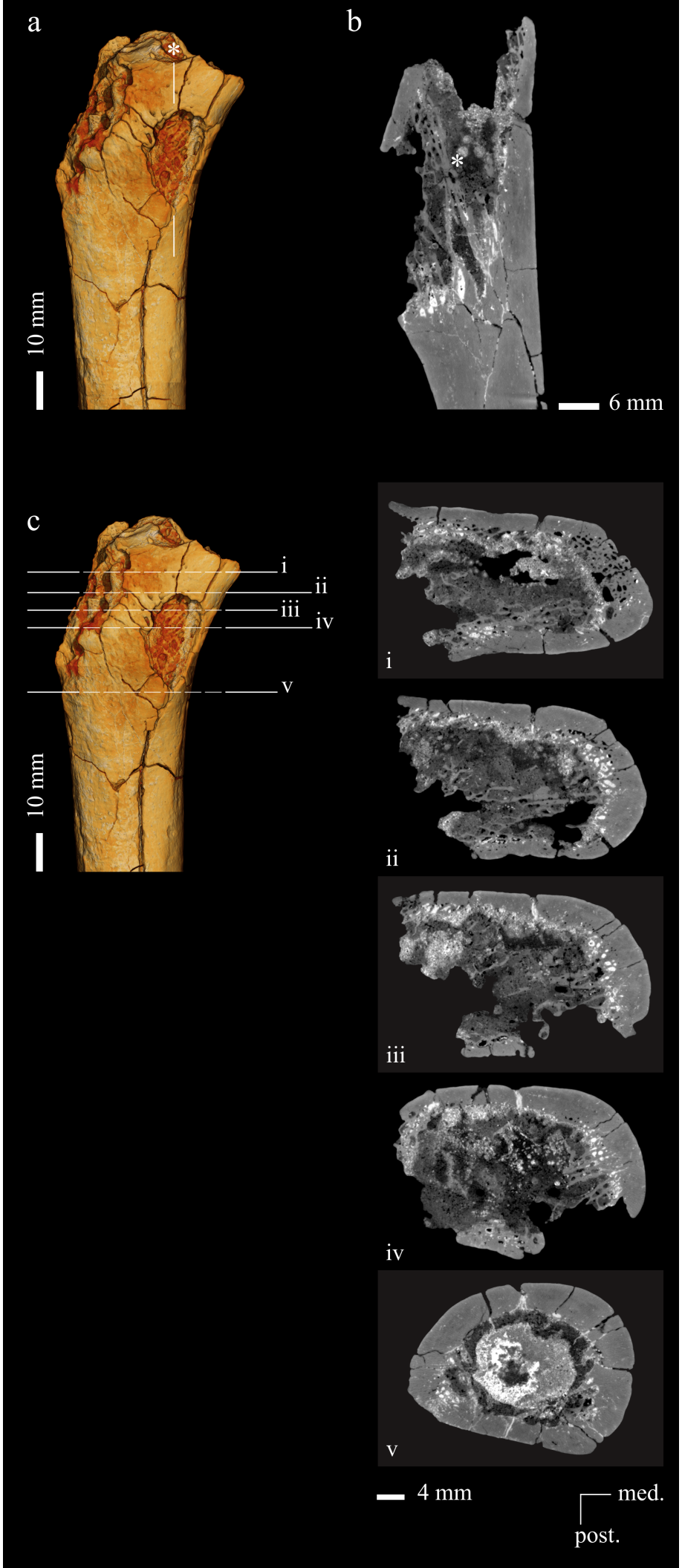
a
10 mm
b
6 mm
c
i
ii
iii
iv
v
10 mm
i
ii
iii
iv
v
4 mm
med.
post.

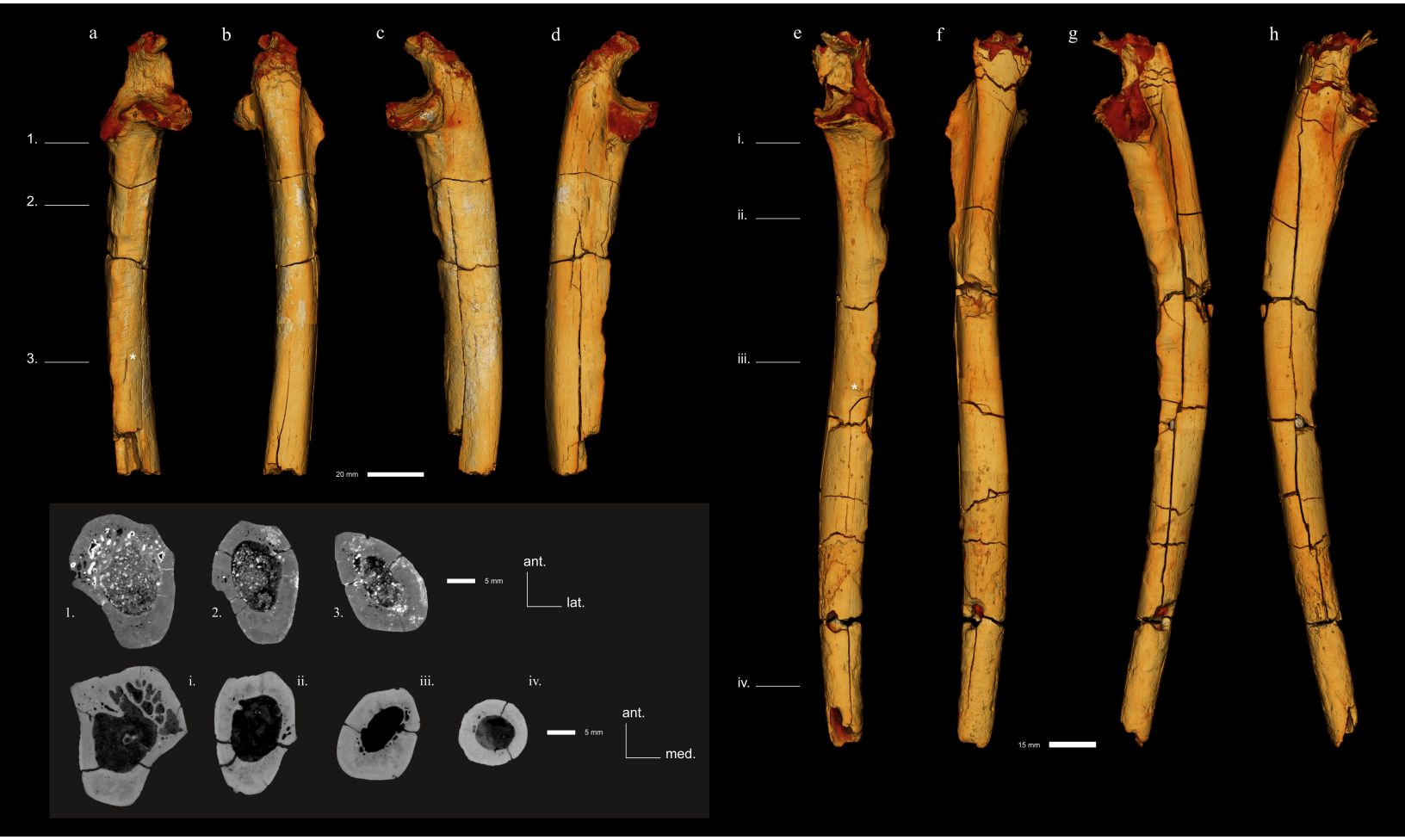
a
b
c
d
e
f
g
h
1.
2.
3.
i.
ii.
iii.
iv.
*
20 mm
15 mm
5 mm
ant.
lat.
med.